5726 *Biochemistry* **2010,** *49,* 5726–5733
DOI: 10.1021/bi100468v

BIOCHEMISTRY
including biophysical chemistry & molecular biology
Article

Kinetics and Morphology of Self-Assembly of an Elastin-like Polypeptide Based on the Alternating Domain Arrangement of Human Tropoelastin[†]

Judith T. Cirulis and Fred W. Keeley*

Molecular Structure and Function Program, Research Institute, The Hospital for Sick Children, and Department of Biochemistry, University of Toronto, 555 University Avenue, Toronto, Ontario, Canada M5G1X8

Received March 30, 2010; Revised Manuscript Received June 8, 2010

ABSTRACT: Elastin is the polymeric extracellular matrix protein responsible for the properties of extensibility and elastic recoil in tissues such as arterial blood vessels, lung parenchyma, and skin. Both tropoelastin (TE), the full-length monomeric form of elastin, and elastin-like polypeptides (ELPs), based on sequences and domain arrangements of TE, have the intrinsic ability to undergo organized self-assembly into network structures through a process of temperature-induced phase separation or coacervation. It has been suggested that this property plays a role in *in vivo* formation of the extracellular elastic matrix. In general, the temperature at which phase separation takes place has been taken as the measure of propensity for self-assembly. However, this phase separation is only the first step in a more complex, multistep process of network formation. We have previously shown that analysis of spectrophotometric data allows extraction of kinetic parameters describing both early (coacervation) and later (maturation) steps of the self-assembly process. Here, using a well-characterized ELP containing three hydrophobic domains flanking two cross-linking domains, we describe the effects of temperature, polypeptide concentration, and solution conditions on the kinetics of self-assembly, providing insights into possible mechanisms for the spontaneous organization of such ELPs into extended networks.

Elastin is the polymeric extracellular matrix protein which is responsible for the properties of extensibility and elastic recoil of many vertebrate tissues, including large arteries, lung parenchyma, and elastic ligaments. Details of the mechanism by which elastic fibers arise from tropoelastin, the monomeric form of elastin, are still under investigation. This process appears to involve interactions with other matrix-associated proteins that form the microfibrillar scaffolding in which polymeric elastin is embedded (*1*−*12*), as well as an intrinsic capacity of tropoelastin for self-aggregation. *In vitro*, even in the absence of any associating proteins, tropoelastin is able to spontaneously form fibrillar structures similar to those seen *in vivo* (*13*−*17*), and it has been proposed that self-assembly of tropoelastin monomers is an early step in the *in vivo* formation of elastic fibers (*15*, *18*, *19*). The self-assembly properties of full-length tropoelastin can also be mimicked by smaller polypeptides and proteins which are modeled after sequences and domain arrangements of this protein (*20*, *21*).

Fundamental to the ability of elastin to self-assemble is its capacity to undergo a thermally induced phase separation, commonly known as coacervation. Coacervation, which occurs upon an elevation of the solution temperature, consists of the formation of a protein-rich second phase and results in a sudden transition from a clear solution to a turbid colloidal suspension. The temperature at which this phase separation occurs is highly reproducible for a given polypeptide or protein and has been shown to be dependent on a number of factors, including ionic strength and pH of the solution, presence of cosolvents, concentration of the polypeptide, number and nature of hydrophobic domains, and characteristics of cross-linking domains (*20*, *22*−*26*).

Coacervation in aqueous solution is not a common property of proteins. The ability of tropoelastin to coacervate is related to its unusual hydrophobic nature, with over 80% of the amino acid residues being nonpolar in character. While the ability of tropoelastin and elastin-like polypeptides to undergo coacervation has been known for years (*13*, *14*, *23*, *27*, *28*), the precise mechanism underlying this behavior is still not understood, although the process must involve a shift in hydration state. Structure of the hydrating water molecules during coacervation is important to consider because coacervation is an entropically driven process in which the increasingly ordered state of the protein is compensated for by the shift of hydrating water molecules into a more disordered state.

In general, the only parameter previously used to characterize the self-assembly of tropoelastin or elastin-like polypeptides (ELPs)[1] has been the temperature at which phase separation or coacervation takes place. However, it is clear that this phase separation is only the initial step in a more complex process through which ordered polymeric structures are generated (*13*, *14*, *21*, *29*−*31*). Using small, well-defined polypeptides modeled on the sequence and domain arrangements of elastin, our laboratory has been investigating factors that affect their coacervation behavior and capacity for formation of ordered polymeric networks (*21*, *20*, *24*, *25*). Recently, we have developed a method involving mathematical analysis of spectrophotometric data which allows extraction of parameters describing both early and later steps of the

[†]This work was supported by an operating grant (T6725) from the Heart and Stroke Foundation of Ontario.
*Corresponding author. Telephone: 416-813-6704. Fax: 416-813-7480. E-mail: fwk@sickkids.ca.

[1]Abbreviations: TE, tropoelastin; ELP, elastin-like polypeptide; TFE, trifluorethanol; Tc, coacervation temperature; Vc, velocity of coacervation; Vm, velocity of maturation.

 Published on Web 06/09/2010

self-assembly process. This was combined with microscopical techniques to visualize coacervate formation and maturation (*32*). Here we used these methods to follow the kinetics of self-assembly of a previously well-characterized elastin-like polypeptide, designated EP20−24−24.

EXPERIMENTAL PROCEDURES

Expression and Purification of EP20−24−24. EP20−24−24 is an elastin-like polypeptide (ELP) containing three hydrophobic domains of human tropoelastin, either exon 20 or 24, interspersed with cross-linking domains consisting of exons 21 and 23 of human tropoelastin, giving the overall domain arrangement 20−21−23−24−21−23−24. Plasmid construction, recombinant expression, purification, and characterization of this polypeptide have been described in detail by Bellingham et al. (*20*, *21*, *24*, *25*). Identity and purity of the final product were confirmed by mass spectrometry and amino acid analysis (Advanced Protein Technology Centre, Hospital for Sick Children, Toronto, Canada) and by the coacervation temperature under defined conditions. Concentration of the ELP was determined by amino acid analysis using norleucine as an internal standard (Advanced Protein Technology Centre, Hospital for Sick Children, Toronto, Canada).

Mathematical Modeling Self-Assembly of EP20−24−24. Spectrophotometric data following the self-assembly of the ELP were collected using a Shimadzu UV-2401PC UV−visible recording spectrophotometer (Mandel Scientific, Guelph, Ontario, Canada) equipped with temperature and stir-rate controllers. Standard coacervation conditions were the following: EP20−24−24 was dissolved on ice to a concentration of 25 μM in 50 mM Tris buffer, pH 7.5, containing 1.5 M NaCl. Sample solutions were equilibrated in a quartz cuvette for 5 min in the spectrophotometer at a temperature approximately 5 °C below the coacervation temperature. A constant stirring rate of 1000 rpm was used except where otherwise indicated. The solution temperature was increased at a rate of 1 °C per minute. Absorbance at 440 nm was automatically recorded every 18 s. After the absorbance reached a maximum, the temperature was held constant for the remainder of the experiment. Data collection was terminated when the absorbance returned to near baseline, defined as approximately 10% of the maximum absorbance, or alternatively after 60 min postcoacervation. Temperature of coacervation, Tc, was measured as the temperature at the onset of increased absorbance (*20*).

For experiments investigating the effect of ionic strength on the kinetics of coacervation, the concentration of the ELP was 0.25 μM and the stirring rate 1000 rpm, as previously described. Concentrations of NaCl varied from 0.75 to 1.5 M. For experiments determining the effect of temperature on kinetics of self-assembly samples were prepared as previously described. The cuvette was then placed in the chamber of the spectrophotometer which had been preheated to a final holding temperature varying between 31 °C (approximately 1 °C above the coacervation temperature under these conditions) and 55 °C. For estimations of activation energy (E_A), lines were fit by linear regression to data points on a plot of ln k (rate constant) vs 1/temperature (K) using Prism 4.0 software (GraphPad Software Inc.). The slope of the lines were taken as $= -E_A R$ (universal gas constant), where $R = 8.3145$ J/(K mol).

Imaging Coacervation and Maturation. Images of polypeptide coacervates were obtained in real time using an Axiovert 200 epifluorescence microscope (Zeiss, Toronto, Ontario, Canada) with a temperature-controlled Attofluor cell chamber (Molecular Probes, Eugene, OR) using conditions that have been described previously (*32*). EP20−24−24 was dissolved in coacervation buffer (50 mM Tris, 1.5 M NaCl, pH 7.5) to a concentration of 200 μM. Images were obtained at various time points for 24 h. The average coacervate droplet sizes were calculated using Volocity 3.6 image analysis software (Improvision, Lexington, MA) after manually defining the edges of the droplets and sampling 60−120 droplets.

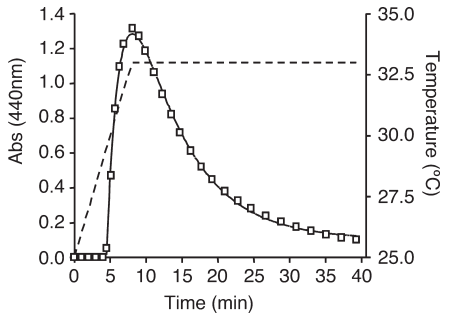

FIGURE 1: Spectrophotometric measurements of changes in turbidity during self-assembly of EP20−24−24. Turbidity was measured using an absorbance of 440 nm (open squares). Details of coacervation conditions are given in the text. The dashed line shows the increase in solution temperature as a function of time. Coacervation temperature, Tc, is the temperature at which coacervation is initiated, approximately 30 °C under these conditions. The solid line is the equation Abs $= -ae^{-k_c t} + be^{-k_m t} + c$ fitted to the absorbance data. Rate constants of coacervation and maturation steps (k_c and k_m) and velocities of the coacervation and maturation steps (Vc and Vm) can be extracted from this fitted curve.

RESULTS

Defining Parameters of Self-Assembly. Similar to observations described previously for other elastin-like polypeptides (*20*, *24*, *25*), when the coacervation temperature for EP20−24−24 was reached, there was a sudden increase in absorption as the sample went from a clear solution to a turbid suspension of colloidal droplets (Figure 1, open squares). This absorption reached a maximum within about 5 min after coacervation and then fell sharply with time to a value of about 10% of the maximum height of the curve. Using Matlab 6.5 (The MathWorks, Natick, MA), a double exponential curve was fit to the changing values of turbidity with time (Figure 1, solid line).

$$\text{absorbance} = -ae^{-k_c t} + be^{-k_m t} + q$$

In this relationship the first term describes the initial rise in turbidity at the onset of phase separation, which we have previously designated as the "coacervation" step of the overall process of self-assembly (*32*). The second term describes the subsequent fall in turbidity with time, a process that we have called "maturation". In this equation, "a" and "b" are concentration proportionality factors, "k_c" and "k_m" are rate constants, and q is the baseline absorption after coacervation. While making no assumptions about mechanism, this relationship resulted in an excellent fit to the turbidity curve (Figure 1, solid line) and allowed the extraction of kinetic parameters of the process, including the velocity of the coacervation step, ak_c (Vc), and the velocity of the maturation step, bk_m (Vm). In this way, Vc, Vm, and the temperature at which coacervation is initiated (Tc) are three parameters that can be used to describe the process of self-assembly for this elastin-like polypeptide.

The fall in turbidity with time during the maturation step was not due to settling of the colloidal droplets, since the sample was constantly stirred in the cuvette (Figure 2). Indeed, stirring had little or no effect on the initiation temperature of coacervation (Tc) or the velocity of coacervation (Vc) but increased Vm, suggesting that the maturation step was diffusion-dependent. Similar results have been reported previously for a different but related elastin-like polypeptide (*32*). Imaging of the coacervation droplets in real time during maturation demonstrated the growth in size of these droplets by coalescence (Figure 3A). The size of the droplets, as measured by their cross-sectional area, initially increased rapidly but subsequently stabilized (Figure 3B).

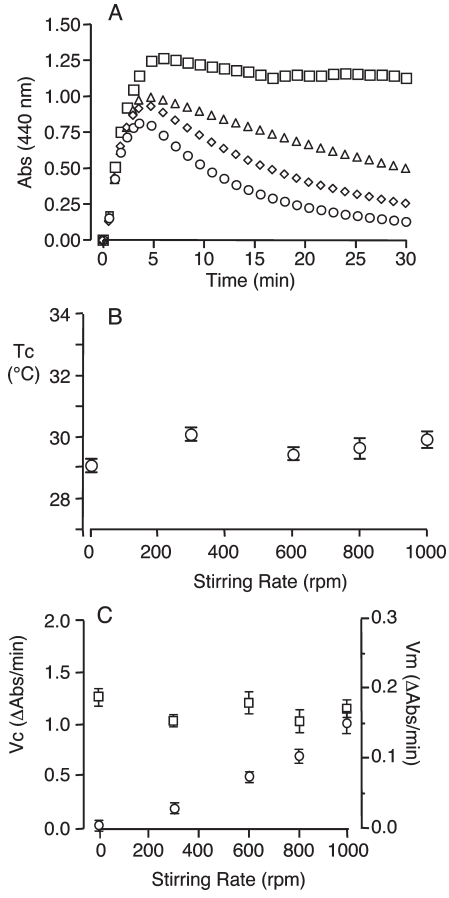

FIGURE 2: Effect of stirring rate on coacervation temperature and kinetic parameters of self-assembly. (A) Increasing stirring rate accelerated the decrease in turbidity with time (squares: 0 rpm; triangles: 300 rpm; diamonds: 600 rpm; circles: 1000 rpm). (B) The temperature of coacervation (Tc) was unaffected by stirring rate. (C) Velocity of the coacervation step (Vc, open squares) was unaffected by stirring, whereas the velocity of the maturation step (Vm, open circles) increased essentially linearly with stirring rate. Mean ± SD, n = 5.

Effect of NaCl on Parameters of Self-Assembly. The effect of salt concentration on coacervation temperature has been well characterized (*20*, *22*). Consistent with those results, coacervation temperature decreased linearly with increasing concentrations of NaCl (Figure 4A), indicating a higher propensity for initiation of phase separation. The velocity of coacervation, Vc, increased significantly with increasing concentrations of NaCl (Figure 4B). In contrast, increased concentrations of NaCl had little or no effect on the velocity of maturation, Vm (Figure 4B). Differential effects of NaCl on coacervation and maturation velocities suggest different mechanisms underlying these two steps of self-assembly.

Effect of Polypeptide Concentration on Parameters of Self-Assembly. Increased concentration of elastin-like polypeptides has previously been shown to lower coacervation temperature (*20*, *23*). Consistent with these observations, the temperature at which the coacervation of EP20−24−24 was initiated decreased in a nonlinear fashion as concentration was increased, with concentration effects particularly strong at lower concentrations (Figure 5A). Both Vc and Vm increased nonlinearly with polypeptide concentration (Figure 5B), with this effect appearing to saturate at higher concentrations. Although both Vc and Vm increased with polypeptide concentration, the magnitude of the effect on Vc was considerably greater than the effect on Vm.

By analogy to the kinetics of reaction mechanisms, the order of a reaction or process can be determined by plotting reaction velocity versus substrate concentration on a double logarithmic plot, with the resulting slope indicating the reaction order. For both coacervation and maturation steps of the self-assembly process of the elastin-like polypeptide, the slope of such a plot showed two components (Figure 5C), suggesting the involvement of a series of linked reactions or processes.

A simple reaction series that would result in velocity changing in a nonlinear relationship to concentration involves three reactions. For example:

$$A \underset{k_2}{\overset{k_1}{\rightleftharpoons}} B \xrightarrow{k_3} C$$

In this case, the reaction product "B" would be an intermediate that could reversibly revert to "A" or proceed to "C". Using this reaction scheme, a relationship between velocity of the overall process, V, and the concentration of the initial substrate "A" can be derived, where "n" is the reaction order.

$$V = \frac{k_1 k_3 [A]^n}{k_2 + k_3 [A]^n}$$

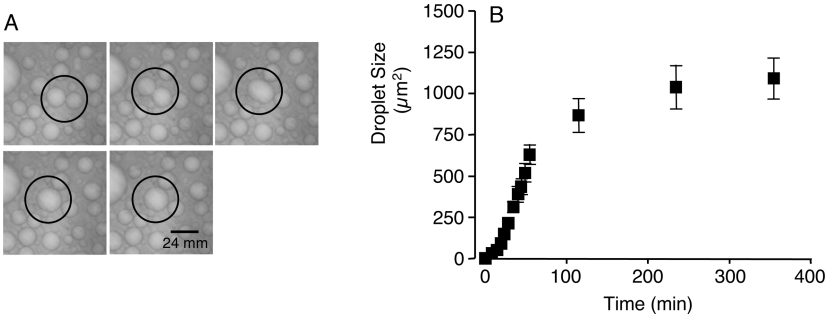

FIGURE 3: Coacervation droplets grew by coalescence during the maturation step. (A) Bright field image series obtained over a period of 1 s shows complete coalescence of two droplets (circled). Scale bar = 24 μm. (B) Mean coacervate droplet size initially increased rapidly, but droplet size stabilized at later times. Mean ± SD, n = 100. Details of methodology for imaging coacervate maturation and measurement of droplet size are given in the text.

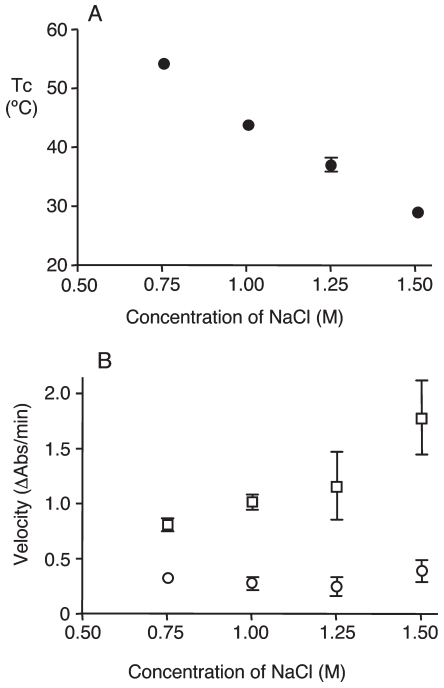

FIGURE 4: Effect of NaCl concentration on coacervation temperature and kinetic parameters of self-assembly. (A) Coacervation temperature (Tc) decreased essentially linearly with increased concentrations of NaCl. (B) Velocity of the coacervation step (Vc, open squares) increased with increasing concentrations of NaCl, whereas the velocity of the maturation step (Vm, open circles) was unaffected. Mean ± SD, $n = 5$.

This relationship was used to fit a curve to the velocity vs ELP concentration data in Figure 5B (solid and dotted lines), allowing a value of "n", representing the order of the process, to be extracted for both coacervation and maturation steps. Determined in this way, $n = 1.3$ for the coacervation step, and $n = 2.0$ for the maturation step. In general, $n > 1$ is characteristic of a sigmoidal curve, describing an overall reaction or process which is cooperative. The maximum velocity of coacervation for EP20−24−24 was 4.0 ΔAbs/min as compared to a maximum velocity of maturation of 0.74 ΔAbs/min.

Effects of Trifluoroethanol (TFE) and Urea on Parameters of Self-Assembly. Increasing concentration of TFE had a strong effect to decrease Tc of EP20−24−24 (Figure 6A), even at relatively low concentrations. This was consistent with previous data on the effects of TFE on other ELPs (*25*, *33*) and tropoelastin (*34*). However, TFE had little or no effect on the velocities of either coacervation, Vc, or maturation, Vm (Figure 6B). In contrast, again consistent with earlier observations (*25*), urea significantly raised the coacervation temperature (Figure 6A). Urea also had a clear effect to decrease the velocity of the coacervation step (Figure 6C). However, the effect of urea on the maturation step appeared to be complex, with a significant increase in Vm at 0.5 M but little effect at higher concentrations.

Effect of Temperature on Kinetics of Self-Assembly. To assess the effect of temperature on kinetic parameters of coacervation and maturation, coacervation was induced by raising the temperature in a single step to various final temperatures, all exceeding the coacervation temperature. Velocity of the coacervation step (Vc) increased essentially linearly with temperature (Figure 7A). In contrast, Vm was also increased with temperature, although this effect plateaued at higher temperatures (Figure 7A). Based on a classic Arrhenius relationship between

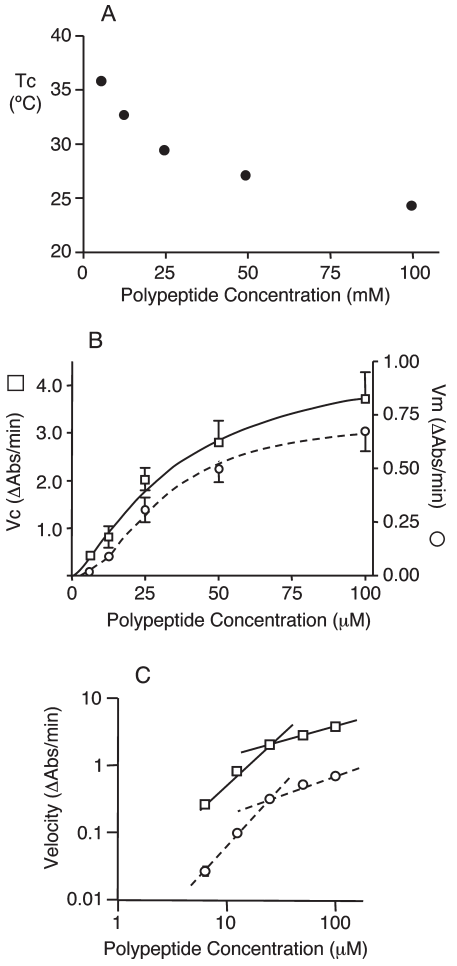

FIGURE 5: Effect of concentration of elastin-like polypeptide (EP20−24−24) on coacervation temperature and kinetic parameters of self-assembly. (A) Coacervation temperature (Tc) decreased nonlinearly with increasing concentrations of polypeptide. (B) Increasing concentrations of polypeptide resulted in nonlinear increases in both velocity of coacervation (Vc, open squares) and velocity of maturation (Vm, open circles). Relationships between polypeptide concentration and Vc (solid line) and Vm (dashed line) were consistent with a simple, two-step reaction mechanism (see text for details). (C) A log−log plot of the effect of polypeptide concentration on reaction velocities showed two components, also consistent with a series of linked reaction steps. Mean ± SD, $n = 5$.

temperature and rate constant, a graph was generated by plotting ln k_c or ln k_m vs $1/T$ (K) (Figure 7B). In such a plot, activation energy of the reaction or process (E_A) can be calculated from the slope of the line according to the relationship

$$E_A = -\text{slope} \times R$$

where R is the universal gas constant and has a value of 8.3145 J/(K mol). From this calculation, the maturation step had a single, very small activation energy of 3.7 kJ/mol (Figure 7B, dotted line). In contrast, the plot for the coacervation step showed two components, with a larger activation energy of 127.0 kJ/mol at temperatures close to the coacervation temperature (Figure 7B, dashed line) and a smaller activation energy of 35.8 kJ/mol at higher temperatures (Figure 7B, solid line). Such nonlinear Arrhenius relationships have previously been associated with proteins undergoing conformational changes (*35*−*37*).

DISCUSSION

In vitro self-assembly of tropoelastin or elastin-like polypeptides is initiated by coacervation, a temperature-induced phase

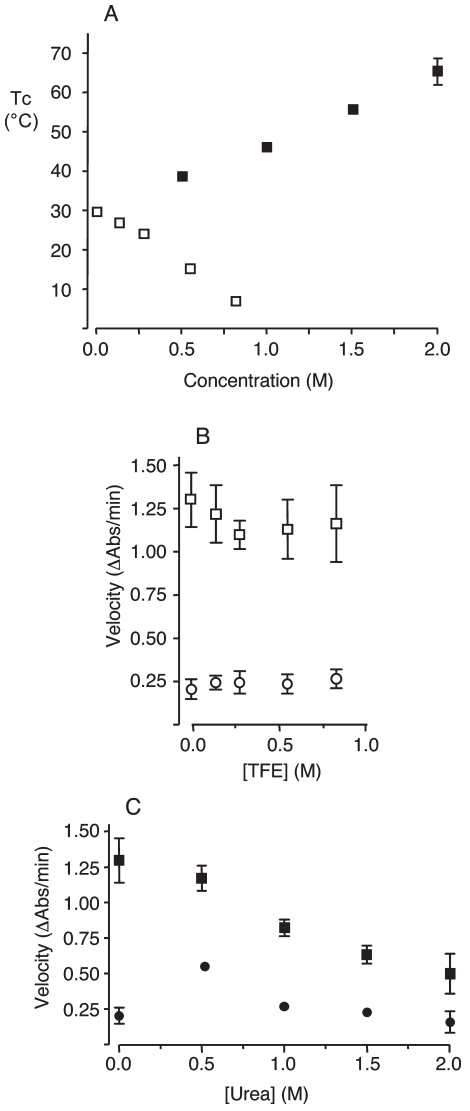

FIGURE 6: Effect of trifluoroethanol (TFE) and urea on coacervation temperature and kinetic parameters of self-assembly. (A) Increasing concentrations of TFE (open squares) decreased coacervation temperature (Tc). In contrast, increasing concentrations of urea (solid squares) increased coacervation temperature. (B) Increasing concentrations of TFE had little or no effect on velocities of either the coacervation (open squares) or the maturation (open circles) step. (C) Increasing concentrations of urea decreased the velocity of the coavervation step (solid squares) but had a less consistent effect on the velocity of the maturation step (solid circles). Mean ± SD, $n = 5$.

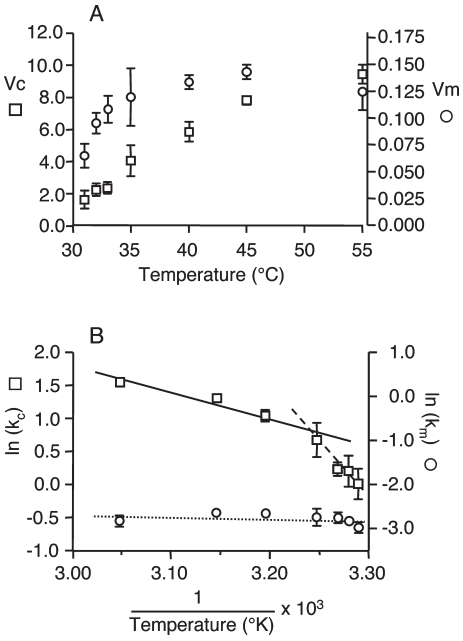

FIGURE 7: Effect of temperature on kinetic parameters of self-assembly. Solutions were held on ice, followed by a single step increase to various final temperatures, all exceeding the coacervation temperature of approximately 30 °C. (A) The velocity of the coacervation step (Vc, open squares) increased linearly with final temperature. In contrast, the velocity of the maturation step (Vm, open circles) showed an exponential increase with final temperature. (B) An Arrhenius plot of the relationships between rate constants of the coacervation (k_c) and maturation (k_m) steps and the final temperature, expressed in kelvin. Activation energies of the steps were calculated from the slopes of the lines (see text for details). For the maturation step, the data could be fit to a single line (dotted), with a slope not significantly different from 0, indicating a very low activation energy. In contrast, the data for the coacervation step showed two distinct components (solid and dashed lines), both with slopes significantly different from 0, indicating two steps with significant but differing activation energies. Mean ± SD, $n = 5$.

separation. The temperature at which this phase separation takes place is called the coacervation temperature, Tc. Several previous studies using similar ELPs that include both hydrophobic and cross-linking domains of human tropoelastin have demonstrated that Tc can be influenced by many factors including solution pH and ionic strength, as well as characteristics of the protein itself, including sequence, overall hydropathy, and domain arrangements (*20*, *22*−*26*). Furthermore, the distribution of polar and apolar regions along the chain of block copolymers modeled on tandem repeats of pentamers of elastin-like sequences has also been shown to be an important determinant of coacervation behavior (*38*).

In general, Tc has been taken to be a measure of the overall propensity of ELPs for self-assembly. However, it is clear that this parameter represents only the susceptibility of the polypeptide to undergo the initial phase separation step of a more complicated multistep process of self-assembly into an organized, extended matrix. We and others have shown that this organized matrix can subsequently be cross-linked into materials with elastomeric properties resembling those of native polymeric elastin (*17*, *21*). While coacervation is classically considered to be reversible upon decreasing solution temperature below Tc, recent rheological data from our laboratory have demonstrated that, even in the absence of cross-linking, holding the coacervate of EP20−24−24 above Tc results in a maturation process in which network formation becomes progressively less reversible with time (*30*).

Several previous studies have described the kinetics of the initiation of coacervation of elastin-like proteins (*6*, *23*, *37*, *39*, *40*). However, most of these have used polypeptides with sequences based only on the hydrophobic domains of elastin (*37*, *39*, *40*). We have previously shown that polypeptides lacking the alternating hydrophobic and cross-linking domain organization of elastin have a much reduced propensity for coacervation (*24*). Furthermore, none of these previous studies have attempted to model postcoacervation events, which include spontaneous organization of the coacervate into an extended network. Here we have used spectrophotometric data to follow the progress of self-assembly beyond the initial phase separation event. Without making any *a priori* assumptions about mechanism, the overall self-assembly process, including both coacervation and maturation steps, can be mathematically modeled using a double exponential curve fit.

In this way, quantitative information on velocities of coacervation and maturation steps can be extracted, providing insights into possible mechanisms of the self-assembly process.

The initial rise in turbidity initiated at the coacervation temperature, referred to here as the coacervation step, was followed by a decrease in turbidity, which we have designated maturation. This decrease in turbidity with time was clearly not due to settling of the colloidal droplets, since increasing stirring rates accelerated maturation. Imaging of the coacervation droplets with time showed that maturation was due to coalescence of droplets, resulting in reduced light scattering from these larger colloidal particles. Temperature of coacervation and rate of the coacervation step were unaffected by stirring. These results were qualitatively similar to those previously reported by us for another ELP, although the rates of the processes differed for the two ELPs (*32*).

Coalescence of colloidal droplets would normally continue until the two phases completely separate into immiscible layers. Indeed, such a process has been described by others using either α-elastin, a heterogeneous mixture of fragments of insoluble polymeric elastin generated by digestion with oxalic acid (*39*), or synthesized polypeptides whose sequences were modeled on hydrophobic domains of elastin (*40*). However, for EP20−24−24 under the conditions described here, coalescence of colloidal droplets ceased after approximately 2 h, and droplet size no longer increased. Similar behavior was previously reported for another related ELP, although the time to achieve a stable droplet and the final droplet size differed (*32*).

Stabilization of colloidal droplets is often achieved by the addition of an exogenous surface-active substance or emulsifier that interacts with the surface of the droplet, inhibiting further coalescence. However, spontaneous stabilization of colloidal droplets in the absence of exogenous stabilizers, the "ouzo effect", has also been described (*41*). An explanation for this spontaneous stabilization of droplet size may be related to progressive development of more extensive intermolecular interactions between the ELPs in the condensed phase. Such behavior would be consistent with the known ability of this type of ELP to form fibrillar networks (*13*−*17*, *30*, *31*). The presence of lysine residues in the cross-linking domains confers an amphiphilic character on the ELP used in this study, and there are several examples in the literature of the formation of stable micelle-like structures by such amphiphilic proteins (*42*, *43*). Alignment of polypeptides at the outer layer of the coacervate droplet/solution interface, with lysines directed toward the solution phase, could result in stabilization of the droplets both by charge−charge repulsion of their surfaces and by providing a template for ordering of polypeptides deeper into the droplet, resulting in the stabilization or rigidification of the surface of the droplets.

Initiation of coacervation clearly reflects a sudden change in the hydration state of the ELP. Given these considerations, the temperature at which coacervation takes place may be related, at least in part, to the stability of water structures surrounding and interacting with the protein in its soluble state. This is consistent with observations of differing susceptibilities to coacervation, reflected in significantly variable coacervation temperatures for ELPs containing similar domain arrangements but different protein sequences (*24*, *25*). Destabilization of these water structures by raising solution temperature would then initiate the process of phase separation. Here we have shown that increasing salt content in solution not only lowers the temperature of coacervation, as has been reported elsewhere by us and others (*20*, *22*, *23*), but also accelerates the coacervation step, presumably reflecting an increased rate of the self-association process which propagates the phase separation. In contrast, the rate of maturation of the coacervate droplets is essentially unaffected by salt concentration.

Coacervation has also been suggested to include a conformational transition in the protein molecule (*44*), although it is not clear whether this conformational change is the cause or the result of the change in hydration state. These conformational changes are generally described as a shift from open polyproline II-like structures stabilized by hydrogen bonding to solvating water, to more closed structures involving type II β-turns stabilized by intramolecular hydrogen bonding (*33*, *37*, *45*−*52*). Trifluoroethanol (TFE) has been widely used as a cosolvent which promotes the formation of intramolecular hydrogen bonds, for example, in the stabilization of α-helical structures in proteins (*53*, *54*). We have previously shown that, even in the absence of effects on α-helical content, low concentrations of TFE have a marked effect to lower coacervation temperature and had proposed that the mechanism for this effect might be through promotion of the conformational shift to closed, β-turn structures, thereby initiating coacervation (*25*). If this were the case, we would expect that TFE should also have a significant effect to increase the velocity of the coacervation step. However, results reported here indicate that concentrations of TFE that have major effects on the coacervation temperature have little or no effect on either rate of coacervation or rate of maturation. This suggests that other mechanisms for the effect of TFE on coacervation temperature may have to be considered (*54*−*56*).

In contrast to TFE, urea is known to destabilize intramolecular hydrogen bonding, including both α-helical and β-turn structures. We had previously shown that increasing concentrations of urea raised coacervation temperatures (*25*). Again, if the self-association step of coacervation requires or is proceeded by formation of β-turn structures in the ELP, we would expect that addition of urea should not only increase the coacervation temperature but also decrease the rate of coacervation, an effect which was consistent with the results reported here. Note that urea, at least at these concentrations, had no effect on the rate of the maturation process.

The effect of polypeptide concentration on coacervation temperature was consistent with previous reports (*20*, *23*). That is, the decrease in coacervation temperature with increased polypeptide concentration was nonlinear, with effects more pronounced at lower concentrations. Velocity of both coacervation and maturation processes showed a nonlinear and saturable dependence on polypeptide concentration, and log−log plots of these relationships suggested that both processes involved multiple, linked substeps. These data could be successfully fit by a mathematical relationship assuming a simple two-step process with a reversible first step, and the calculated orders of these processes were consistent with cooperative kinetics. In the case of coacervation, this first, reversible substep may be related to the change in ELP conformation discussed above, while the second substep could correspond to the subsequent process of molecular self-association to form the initial coacervate droplets. It is more difficult to account for the predicted multistep nature of the maturation process, although in that case the substeps could reflect the initial rapid coalescence of the droplets followed by their stabilization.

The effect of temperature on a reaction rate or process can also provide information on its nature. Our data have shown that the

temperature at which coacervation was induced affected both coacervation and maturation rates, although these two processes appeared to have different kinetic characteristics. An Arrhenius plot of these data indicated a very low activation energy of approximately 3.7 kJ/mol (0.88 kcal/mol) for the maturation step, which was constant over the entire temperature range, suggesting that this process was essentially spontaneous. In contrast, the Arrhenius plot of the coacervation rate was nonlinear, with regions corresponding to two distinct slopes. At temperatures close to the coacervation temperature, 30 °C under the conditions used, the activation energy was high, approximately 127 kJ/mol (30.3 kcal/mol). At higher temperatures the activation energy of the coacervation step fell to approximately 35.8 kJ/mol (8.5 kcal/mol). A temperature-dependent change in activation energy has also been reported for coacervation of an elastin-like protein consisting of mutiple repeats of the hydrophobic PGVGV sequences (*37*), with an initial E_A of 537 kJ/mol and a subsequent *E*A of 380 kJ/mol. Higher activation energies for a ELP containing only hydrophobic domains, as compared to the ELP reported here, are consistent with our earlier observations that the alternating domain organization of tropoelastin strongly increases propensity for coacervation (*24*). These data are also consistent with a two-step process of coacervation.

Both experimental and computational modeling data suggest an equilibrium between open and closed conformations of ELPs, which is shifted toward increasing the proportion of closed conformations as dehydration of the polypeptide takes place by increasing temperature or other alterations in solution conditions (*33*, *45*−*52*). If such closed conformations are required for molecular self-association, this would suggest that the coacervation temperature represents the temperature at which a critical concentration of these closed conformations has been reached, permitting propagation of molecular association events and leading to the appearance of the macroscopic coacervation droplets. Consistent with experimental data, this critical concentration of closed conformations would be affected by factors such as polypeptide concentration, solution ionic strength, agents such as TFE or urea which influence water−polypeptide interactions or intramolecular hydrogen bond stability, and the sequence of the ELP itself. In the model of the coacervation stage of self-assembly described here, the conformational change in the ELP would correspond to an initial substep with high activation energy, while propagation of the molecular association events to form the coacervation droplets would be represented by a second, lower activation energy substep.

The coacervation droplets, once formed, initially grow by coalescence, accounting for the fall in turbidity of the colloidal suspension, its apparent dependence on diffusion, and the very low activation energy of this maturation process. However, at least for the types of ELPs described here which mimic the alternating domain arrangement of elastin, such coalescence does not proceed to complete phase separation. Instead, droplets reach a stable size as coalescence ceases. Knowing the propensity of these polypeptides to form organized structures, we postulate that cessation of droplet growth for these ELPs may be related to an organization of the polypeptides at the interfacial surface, effectively inhibiting the ability of the droplets to grow by coalescence.

In summary, using a simple mathematical analysis of spectrophotometric data, we have been able to expand the parameters used to describe self-assembly of ELPs to include not only the temperature at which the initial phase separation takes place but also the kinetics of the coacervation and maturation steps in the overall self-assembly process. The data show clearly that these three parameters can be independently influenced by solution conditions and confirm that the temperature at which coacervation takes place is not necessarily a sufficient measure of the overall propensity of such polypeptides for self-assembly. Furthermore, the results reported here, together with data from others using a variety of experimental and computational techniques, suggest an overall model for self-assembly which would apply at least to such simple ELPs and may also have relevance for understanding the self-assembly of native tropoelastin both *in vitro* and *in vivo*.

REFERENCES

1. Trask, T. M., Trask, B. C., Ritty, T. M., Abrams, W. R., Rosenbloom, J., and Mecham, R. P. (2000) Interaction of tropoelastin with the amino-terminal domains of fibrillin-1 and fibrillin-2 suggests a role for the fibrillins in elastic fiber assembly. *J. Biol. Chem. 275*, 24400–24406.
2. Jensen, S. A., Reinhardt, D. P., Gibson, M. A., and Weiss, A. S. (2001) Protein interaction studies of MAGP-1 with tropoelastin and fibrillin-1. *J. Biol. Chem. 276*, 39661–39616.
3. Nakamura, T., Lozano, P. R., Ikeda, Y., Iwanaga, Y., Hinek, A., Minamisawa, S., Cheng, C. F., Kobuke, K., Dalton, N., Takada, Y., Tashiro, K., Ross, J., Jr., Honjo, T., and Chien, K. R. (2002) Fibulin-5/DANCE is essential for elastogenesis *in vivo*. *Nature 415*, 171–175.
4. Reinboth, B., Hanssen, E., Cleary, E. G., and Gibson, M. A. (2002) Molecular interactions of biglycan and decorin with elastic fiber components: biglycan forms a ternary complex with tropoelastin and microfibril-associated glycoprotein 1. *J. Biol. Chem. 277*, 3950–3957.
5. Yanagisawa, H., Davis, E. C., Starcher, B. C., Ouchi, T., Yanagisawa, M., Richardson, J. A., and Olson, E. N. (2002) Fibulin-5 is an elastin-binding protein essential for elastic fiber development *in vivo*. *Nature 415*, 168–171.
6. Clarke, A. W., Wise, S. G., Cain, S. A., Kielty, C. M., and Weiss, A. S. (2005) Coacervation is promoted by molecular interactions between the PF2 segment of fibrillin-1 and the domain 4 region of tropoelastin. *Biochemistry 44*, 10271–10281.
7. Hirai, M., Ohbayashi, T., Horiguchi, M., Okawa, K., Hagiwara, A., Chien, K. R., Kita, T., and Nakamura, T. (2007) Fibulin-5/DANCE has an elastogenic organizer activity that is abrogated by proteolytic cleavage *in vivo*. *J. Cell Biol. 176*, 1061–1071.
8. Zheng, Q., Davis, E. C., Richardson, J. A., Starcher, B. C., Li, T., Gerard, R. D., and Yanagisawa, H. (2007) Molecular analysis of fibulin-5 function during de novo synthesis of elastic fibers. *Mol. Cell. Biol. 27*, 1083–1095.
9. Lemaire, R., Bayle, J., Mecham, R. P., and Lafyatis, R. (2007) Microfibril-associated MAGP-2 stimulates elastic fiber assembly. *J. Biol. Chem. 282*, 800–808.
10. Brown-Augsburger, P., Broekelmann, T., Rosenbloom, J., and Mecham, R. P. (1996) Functional domains on elastin and microfibril-associated glycoprotein involved in elastic fiber assembly. *Biochem. J. 318*, 149–155.
11. Trask, B. C., Trask, T. M., Broekelmann, T., and Mecham, R. P. (2000) The microfibrillar proteins MAGP-1 and fibrillin-1 form a ternary complex with the chondroitin sulfate proteoglycan decorin. *Mol. Biol. Cell 11*, 1499–1507.
12. Wachi, H., Nonaka, R., Sato, F., Shibata-Sato, K., Ishida, M., Iketani, S., Maeda, I., Okamoto, K., Urban, Z., Onoue, S., and Seyama, Y. (2008) Characterization of the molecular interaction between tropoelastin and DANCE/fibulin-5. *J. Biochem. 143*, 633–639.
13. Cox, B. A., Starcher, B. C., and Urry, D. W. (1974) Coacervation of tropoelastin results in fiber formation. *J. Biol. Chem. 249*, 997–998.
14. Bressan, G. M., Castellani, I., Giro, M. G., Volpin, D., Fornieri, C., and Pasquali Ronchetti, I. (1983) Banded fibers in tropoelastin coacervates at physiological temperatures. *J. Ultrastruct. Res. 82*, 335–340.
15. Bressan, G. M., Pasquali-Ronchetti, I., Fornieri, C., Mattioli, F., Castellani, I., and Volpin, D. (1986) Relevance of aggregation properties of tropoelastin to the assembly and structure of elastic fibers. *J. Ultrastruct. Mol. Struct. Res. 94*, 209–216.
16. Bedell-Hogan, D., Trackman, P., Abrams, W., Rosenbloom, J., and Kagan, H. (1993) Oxidation, cross-linking, and insolubilization of recombinant tropoelastin by purified lysyl oxidase. *J. Biol. Chem. 268*, 10345–10350.

17. Mithieux, S. M., Rasko, J. E., and Weiss, A. S. (2004) Synthetic elastin hydrogels derived from massive elastic assemblies of self-organized human protein monomers. *Biomaterials 25*, 4921–4927.
18. Kozel, B. A., Rongish, B. J., Czirok, A., Zach, J., Little, C. D., Davis, E. C., Knutsen, R. H., Wagenseil, J. E., Levy, M. A., and Mecham, R. P. (2006) Elastic fiber formation: a dynamic view of extracellular matrix assembly using timer reporters. *J. Cell. Physiol. 207*, 87–96.
19. Czirok, A., Zach, J., Kozel, B. A., Mecham, R. P., Davis, E. C., and Rongish, B. J. (2006) Elastic fiber macro-assembly is a hierarchical, cell motion-mediated process. *J. Cell. Physiol. 207*, 97–106.
20. Bellingham, C. M., Woodhouse, K. A., Robson, P., Rothstein, S. J., and Keeley, F. W. (2001) Self-aggregation characteristics of recombinantly expressed human elastin polypeptides. *Biochim. Biophys. Acta 1550*, 6–19.
21. Bellingham, C. M., Lillie, M. A., Gosline, J. M., Wright, G. M., Starcher, B. C., Bailey, A. J., Woodhouse, K. A., and Keeley, F. W. (2003) Recombinant human elastin polypeptides self-assemble into biomaterials with elastin-like properties. *Biopolymers 70*, 445–455.
22. Luan, C. H., Parker, T. M., Prasad, K. U., and Urry, D. W. (1991) Differential scanning calorimetry studies of NaCl effect on the inverse temperature transition of some elastin-based polytetra-, polypenta-, and polynonapeptides. *Biopolymers 31*, 465–475.
23. Vrhovski, B., Jensen, S., and Weiss, A. S. (1997) Coacervation characteristics of recombinant human tropoelastin. *Eur. J. Biochem. 250*, 92–98.
24. Miao, M., Bellingham, C. M., Stahl, R. J., Sitarz, E. E., Lane, C. J., and Keeley, F. W. (2003) Sequence and structure determinants for the self-aggregation of recombinant polypeptides modeled after human elastin. *J. Biol. Chem. 278*, 48553–48562.
25. Miao, M., Cirulis, J. T., Lee, S., and Keeley, F. W. (2005) Structural determinants of cross-linking and hydrophobic domains for self-assembly of elastin-like polypeptides. *Biochemistry 44*, 14367–14375.
26. Reguera, J., Urry, D. W., Parker, T. M., McPherson, D. T., and Rodriguez-Cabello, J. C. (2007) Effect of NaCl on the exothermic and endothermic components of the inverse temperature transition of a model elastin-like polymer. *Biomacromolecules 8*, 354–358.
27. Cox, B. A., Starcher, B. C., and Urry, D. W. (1973) Coacervation of alpha-elastin results in fiber formation. *Biochim. Biophys. Acta 317*, 209–213.
28. Urry, D. W., and Long, M. M. (1977) On the conformation, coacervation and function of polymeric models of elastin. *Adv. Exp. Med. Biol. 79*, 685–714.
29. Clarke, A. W., Arnspang, E. C., Mithieux, S. M., Korkmaz, E., Braet, F., and Weiss, A. S. (2006) Tropoelastin massively associates during coacervation to form quantized protein spheres. *Biochemistry 45*, 9989–9996.
30. Cirulis, J. T., and Keeley, F. W. (2009) Viscoelastic properties and gelation of an elastin-like polypeptide. *J. Rheol. 53*, 1215–1228.
31. Tu, Y., Wise, S. G., and Weiss, A. S. (2010) Stages in tropoelastin coalescence during synthetic elastin hydrogel formation. *Micron 41*, 268–272.
32. Cirulis, J. T., Bellingham, C. M., Davis, E. C., Hubmacher, D., Reinhardt, D. P., Mecham, R. P., and Keeley, F. W. (2008) Fibrillins, fibulins, and matrix-associated glycoprotein modulate the kinetics and morphology of *in vitro* self-assembly of a recombinant elastin-like polypeptide. *Biochemistry 47*, 12601–12613.
33. Pepe, A., Guerra, D., Bochicchio, B., Quaglino, D., Gheduzzi, D., Pasquali Ronchetti, I., and Tamburro, A. M. (2005) Dissection of human tropoelastin: supramolecular organization of polypeptide sequences coded by particular exons. *Matrix Biol. 24*, 96–109.
34. Muiznieks, L. D., Jensen, S. A., and Weiss, A. S. (2003) Structural changes and facilitated association of tropoelastin. *Arch. Biochem. Biophys. 410*, 317–323.
35. Scalley, M. L., and Baker, D. (1997) Protein folding kinetics exhibit an Arrhenius temperature dependence when corrected for the temperature dependence of protein stability. *Proc. Natl. Acad. Sci. U.S.A. 94*, 10636–10640.
36. Schreiner, E., Nicolini, C., Ludolph, B., Ravindra, R., Otte, N., Kohlmeyer, A., Rousseau, R., Winter, R., and Marx, D. (2004) Folding and unfolding of an elastin-like oligopeptide: "inverse temperature transition," reentrance, and hydrogen-bond dynamics. *Phys. Rev. Lett. 92*, 148101-1–148101-4.
37. Reguera, J., Lagaron, J. M., Alonso, M., Reboto, V., Calvo, B., and Rodriguez-Cabello, J. C. (2003) Thermal behavior and kinetic analysis of the chain unfolding and refolding and of the concomitant nonpolar solvation and desolvation of two elastin-like polymers. *Macromolecules 36*, 8470–8476.
38. Ribeiro, A., Arias, F. J., Reguera, J., Alonso, M., and Rodriguez-Cabello, J. C. (2009) Influence of the amino-acid sequence on the inverse temperature transition of elastin-like polymers. *Biophys. J. 97*, 312–320.
39. Zhang, Y., Mao, H., and Cremer, P. S. (2003) Probing the mechanism of aqueous two-phase system formation for alpha-elastin on-chip. *J. Am. Chem. Soc. 125*, 15630–15635.
40. Zhang, Y., Trabbic-Carlson, K., Albertorio, F., Chilkoti, A., and Cremer, P. S. (2006) Aqueous two-phase system formation kinetics for elastin-like polypeptides of varying chain length. *Biomacromolecules 7*, 2192–2199.
41. Vitale, S. A., and Katz, J. L. (2003) Liquid droplet dispersions formed by homogeneous liquid-liquid nucleation: "the ouzo effect. *Langmuir 19*, 4105–4110.
42. Nichols, M. R., Moss, M. A., Reed, D. K., Hoh, J. H., and Rosenberry, T. L. (2005) Rapid assembly of amyloid-β peptide at a liquid/liquid interface produces unstable β-sheet fibers. *Biochemistry 44*, 165–173.
43. Dreher, M. R., Simnick, A. J., Fischer, K., Smith, R. J., Patel, A., Schmidt, M., and Chilkoti, A. (2008) Temperature triggered self-assembly of polypeptides into multivalent spherical micelles. *J. Am. Chem. Soc. 130*, 687–694.
44. Yamaoka, T., Tamura, T., Seto, Y., Tada, T., Kunugi, S., and Tirrell, D. A. (2003) Mechanism for the phase transition of a genetically engineered elastin model peptide (VPGIG)40 in aqueous solution. *Biomacromolecules 4*, 1680–1685.
45. Kurková, D., Kríz, J., Schmidt, P., Dybal, J., Rodríguez-Cabello, J. C., and Alonso, M. (2003) Structure and dynamics of two elastin-like polypentapeptides studied by NMR spectroscopy. *Biomacromolecules 4*, 589–601.
46. Li, B., and Daggett, V. (2003) The molecular basis of the temperature- and pH-induced conformational transitions in elastin-based peptides. *Biopolymers 68*, 121–129.
47. Tamburro, A. M., Bochicchio, B., and Pepe, A. (2003) Dissection of human tropoelastin: exon-by-exon chemical synthesis and related conformational studies. *Biochemistry 42*, 13347–13362.
48. Bochicchio, B., Floquet, N., Pepe, A., Alix, A. J., and Tamburro, A. M. (2004) Dissection of human tropoelastin: solution structure, dynamics, and self-assembly of the exon 5 peptide. *Chemistry 10*, 3166–3176.
49. Rousseau, R., Schreiner, E., Kohlmeyer, A., and Marx, D. (2004) Temperature-dependent conformational transitions and hydrogen-bond dynamics of the elastin-like octapeptide GVG(VPGVG): a molecular-dynamics study. *Biophys. J. 86*, 1393–1407.
50. Pepe, A., Guerra, D., Bochicchio, B., Quaglino, D., Gheduzzi, D., Pasquali Ronchetti, I., and Tamburro, A. M. (2005) Dissection of human tropoelastin: supramolecular organization of polypeptide sequences coded by particular exons. *Matrix Biol. 24*, 96–109.
51. Rauscher, S., Baud, S., Miao, M., Keeley, F. W., and Pomès, R. (2006) Proline and glycine control protein self-organization into elastomeric or amyloid fibrils. *Structure 14*, 1667–1676.
52. Krukau, A., Brovchenko, I., and Geiger, A. (2007) Temperature-induced conformational transition of a model elastin-like peptide GVG(VPGVG)(3) in water. *Biomacromolecules 8*, 2196–2202.
53. Sönnichsen, F. D., Van Eyk, J. E., Hodges, R. S., and Sykes, B. D. (1992) Effect of trifluoroethanol on protein secondary structure: an NMR and CD study using a synthetic actin peptide. *Biochemistry 31*, 8790–8798.
54. Buck, M. (1998) Trifluoroethanol and colleagues: cosolvents come of age. Recent studies with peptides and proteins. *Q. Rev. Biophys. 31*, 297–355.
55. Kentsis, A., and Sosnick, T. R. (1998) Trifluoroethanol promotes helix formation by destabilizing backbone exposure: desolvation rather than native hydrogen bonding defines the kinetic pathway of dimeric coiled coil folding. *Biochemistry 37*, 14613–14622.
56. Reiersen, H., and Rees, A. R. (2000) Trifluoroethanol may form a solvent matrix for assisted hydrophobic interactions between peptide side chains. *Protein Eng. 13*, 739–743.